Int. J. Multiphase Flow Vol. 12, No. 3, pp. 445–458, 1986
Printed in Great Britain

0301–9322/86 $3.00+.00
Pergamon Journals/Elsevier

SOLID PARTICLE VELOCITY IN VERTICAL GASEOUS SUSPENSION FLOWS

SHIGERU MATSUMOTO, HIROMI HARAKAWA, MUTSUMI SUZUKI and SHIGEMORI OHTANI
Department of Chemical Engineering, Tohoku University, Sendai 980, Japan

(*Received* 21 *February* 1985; *in revised form* 22 *August* 1985)

Abstract—An optical method, which is based on cross-correlating the signals of two photo-sensors, is applied to measure the average velocity of solid particles transported vertically by a turbulent air stream. Particle velocities measured by the method showed two interesting features; the relative velocity was smaller than the terminal velocity of a single particle at lower air velocities but greater at higher velocities, and for smaller sizes of particles it tended to depend on the solid concentration as well. An empirical correlation was presented for the average particles velocity and tested with literature data. The average drag coefficients, which were evaluated indirectly from the measured relative velocities and the pressure drop due to solids alone, exhibited significant increase compared with the standard ones.

1. INTRODUCTION

There are many industrial processes which involve gas–solid two-phase flow systems besides pneumatic conveyer. Typical applications are fluid catalytic cracking, coal combustion and gasification, pneumatic drying, and flash smelting of copper concentrates. In the optimum design and/or operation of such processes, a knowledge of the solid particle velocity or concentration in the transport line is required; for instance, to calculate the optimum gas velocity for stable operation (e.g. Matsumoto *et al.* 1982), the pressure drop, and the residence time of solids.

Considerable efforts, therefore, have been devoted to this subject in theoretical and experimental aspects. Unfortunately, no unified and accurate approach has been established yet. It is still difficult to predict an accurate solid particle velocity for a given set of operating parameters. This is mainly due to the complex mechanism of the gas–solid two-phase system, such as particle–particle, particle–gas, and particle–wall interactions, which are difficult to be isolated experimentally. Hence progress in theoretical investigation has been slow. In addition, little experimental work has been published because of difficulties in developing accurate methods of measurement of particle velocity.

The principal measuring principles having been used up to now are (1) photographic measurement (Konno & Saito 1969; Reddy & Pei 1969), (2) direct measurement of solid hold-up by quick-closing valve technique (Capes & Nakamura 1973; Hariu & Molstad 1949), (3) electro-capacitance technique (Beck *et al.* 1969; Irons & Chang 1983), and (4) laser-Doppler anemometry (Lee & Srinivansan 1978, 1982). The photographic method is restricted to a very dilute concentration range. The second method has a danger of disturbing the suspension flow itself. Both of them are not available to on-line measurement. The third method is capable of *in situ* measurement, but is rather inferior in the accuracy. The laser-Doppler anemometry is the most reliable technique, at the present time, to measure local velocity distribution of particles and covers a wide variety of gaseous suspension flow. The only weakness is of too high cost to be provided for actual implementation.

In this work, a nonintrusive optical method is developed by means of cross-correlation technique, and average velocities of solid particles are measured in a fully developed region of vertical gaseous suspensions. A similar optical method has recently been applied to gas–liquid two-phase flow (Lübbesmeyer & Leoni 1983). The common advantage of such optical method is the low cost, high precision, and further applicability to on-line measurement for process control. In the latter half of this paper, we are concerned with the correlation of particle velocity and with drag coefficient of suspension, which are evaluated by the use of observed particle velocities.

2. EXPERIMENTAL APPARATUS AND PROCEDURES

2.1 Apparatus

2.1.1 Outline of system. The schematic diagram of an experimental system is shown in figure 1, which is a pressure-type conveying system consisting of a test line of a 20 mm-I.D. Pyrex glass tube of 5.6 m length. Flow rate of air, supplied by a rotary blower, is controlled by an electromotive valve and measured by an orifice-meter. Solid particles are fed by a vibrating feeder with a variable-speed motor. Flow rate of solids is measured by means of a handmade impact flow-meter consisting of a small-sized load-cell. Pressures at various locations along the line and the pressure difference at the orifice-meter are measured by means of semiconductor pressure transducer via a scanning valve. The particle velocity is measured at the location of 4 m up from the solid feed point, where the suspension flow is fully developed. This was confirmed in the preliminary experiment.

The solid particles used in this experiment are spherical particles the physical properties of which are summarized in table 1.

2.1.2 Photo-sensors. The optical sensor consists of two pairs of photo-diode and photo-transistor, which are about 1 cm apart from each other, as shown in figure 2. The photo-diode and -transistor used here are, respectively, TLN101 (its peak wavelength is 9400A) and TPS601. They are selected from the standpoint of high directivity and sensitivity. The output signals (weak current) of detectors are converted to DC voltage and then amplified by an operational amplifier (LM-301A). The size of light-beams and the distance between them were determined through the preliminary experiment, in which the output signals were examined by traversing a fine probe (diameter of 0.7 mm) across the photo-sensing part arranged, as shown in figure 3, in the same way as in the transport line. The result is also illustrated in figure 3. It can be seen that the sensible size of each light-beam is less than 3 mm and the distance of peak to peak is 9.9 mm.

2.2 Procedures

2.2.1 Measuring principle of particle velocity. To explain the method, as an example, the time-dependent fluctuations of the output signals from two light-beam detectors are shown in figure 4. The fluctuations are due to the intercepts of particles across the light-beam

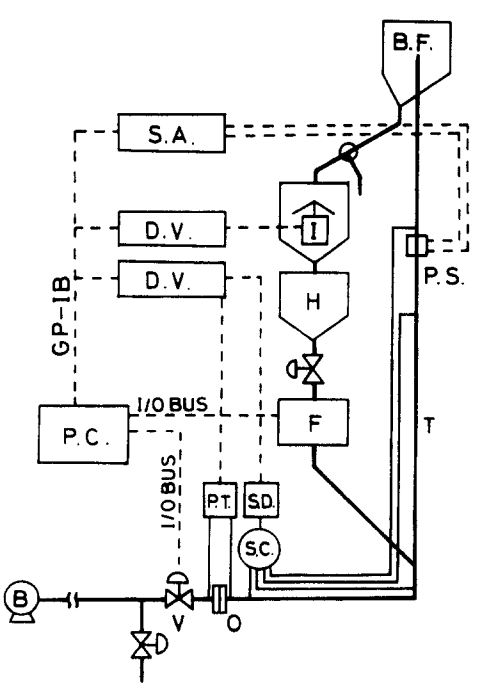

Figure 1. Experimental system. B—rotary blower; B.F.—bag-filter; D.V.—digital voltmeter; F—feeder; H—hopper; I—impact flow-meter; O—orifice meter; P.C.—personal computer; P.S.—photo-sensor; P.T.—pressure transducer; S.A.—signal analyzer; S.C.—scanning valve; S.D.—scanning valve driver; T—test pipe; V—control valve.

Table 1. Properties of solid particles

Material	ρ_p [kg/m^3]	d_p (Sauter mean) [mm]	Standard deviation* [mm]	u_t** [m/s]	$d_p u_t / \nu$ [–]	Fr_t [–]	Key
Glass	2500	0.52	0.047	3.9	136	8.8	○
		1.02	0.106	7.1	483	16.0	△
		1.91	0.169	10.9	1389	24.6	□
		2.93	0.264	14.0	2741	31.7	▽
Copper	8700	0.21	0.038	3.7	51	8.2	●
		0.47	0.063	7.8	243	17.7	▲

* Standard deviations were based on the number median diameter.
**Terminal velocities were calculated by use of Sauter mean diameter.

from the photo-diode. The measurement was carried out in a relatively dilute concentration of solids with the 2.93 mm glass beads. The upper signal is that of the upstream detector; the lower, is that of the downstream one. As can be easily seen, the signal-patterns of the two detectors are very similar but a certain time-shift can be recognized, in this special case, even directly from the signals. In the usual cases, however, the situation is more complicated and it is not so easy to recognize the transit-time from the two signal-traces. Statistical average value of the transit-time, in such cases, can be evaluated from the cross-correlation function which describes the similarity of two-signals ($x(t)$ and $y(t)$) as a function of time-delay τ between them; expressed mathematically,

$$R_{xy}(\tau) = \int_{-\infty}^{\infty} x(t) \cdot y(t-\tau) dt \,. \qquad [1]$$

The cross-correlation function of the example signals in figure 4 is shown in the same figure. It obviously indicates a maximum at the delay-time τ_p. Accordingly, the average transit-time of the particle is related to the maximum of the cross-correlation function. The calculation of the cross-correlation function is performed in an intelligent signal-analyzer (Iwatsu Model SM2100A), where the cross-correlation function is obtained by use of inverse Fourier transform of the cross-spectrum function based on the FFT algorithm. The sampling interval of the signals was chosen as 24 or 48 μ s, depending on the particle size and the flow rate of solids, so that the Nyquist frequency exceeded the expected maximum frequency embedded in the fluctuations. The number of sampled data of each signal was 4096 from the restriction of memory in the signal analyzer. In order to raise the accuracy, the cross-correlation function was estimated, in this work, by averaging 20 measurements of it and then the mean delay-time τ_p was obtained, which all were performed in the signal analyzer. Through this procedure, the maximum peak of the cross-correlation can be made much clearer. The limit of measurement by this method is up to the high solid concentration in which the recirculation of solids occurs in the transport line. For example, figure 5 shows the variation of the cross-correlation functions as an air flow rate was reduced at a constant

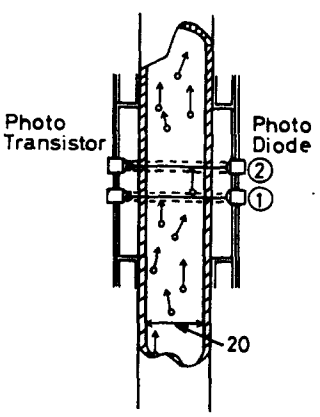

Figure 2. Photo-sensors.

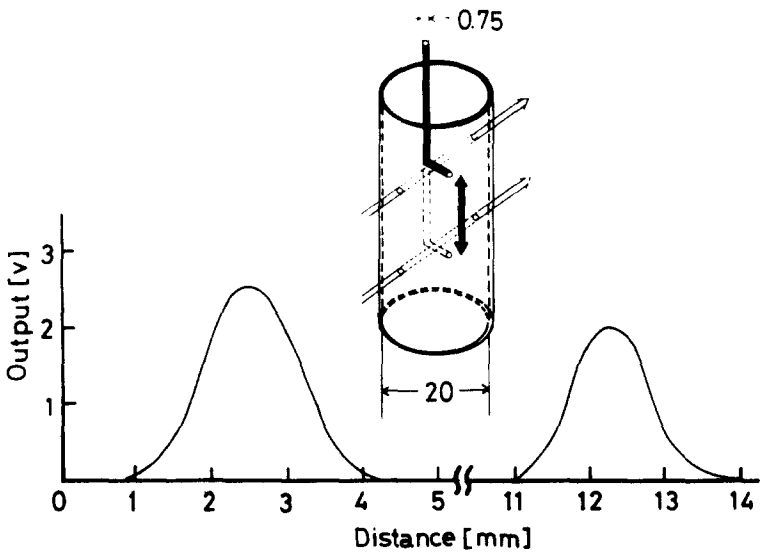

Figure 3. Calibration of photo-sensors.

solids flow rate. It can be seen that the delay-time τ_p increases with decrease in the air flow rate and then the particle velocity becomes slower. In this case, at the air velocity of 8.48 m/s, the solid particles exhibited recirculations and the flow state was at the so-called slug flow.

The results by this method were checked by the usual photographic method by use of a strobo flash, though it was limited to the cases of larger sized particles. The comparisons between them are illustrated in figure 6, which exhibits a good agreement. It should be noted that the photo-sensor used in the present method is of very low cost and the measurement can be done in very short time if an FFT analyzer is used. Therefore, this technique has the possibility of application to on-line measurement.

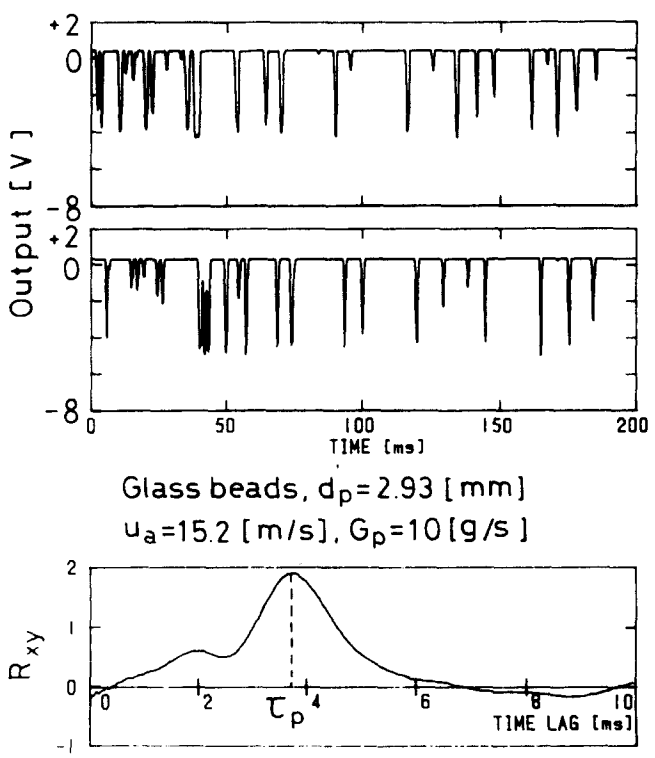

Figure 4. Example of output signals of photo-sensors and cross-correlation function.

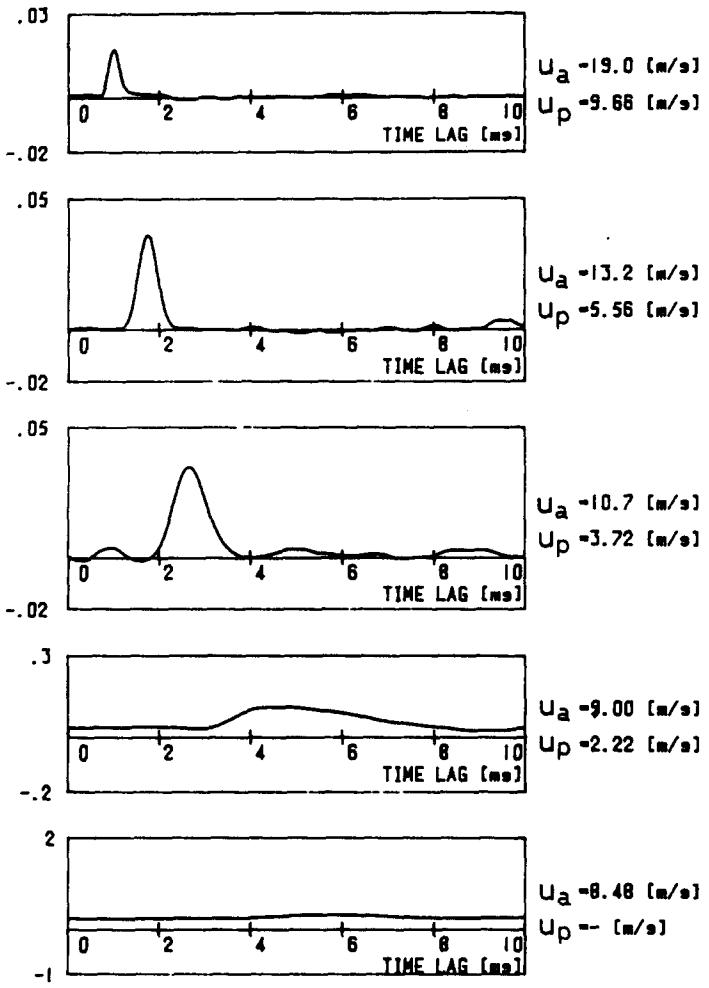

5. Variation of cross-correlation functions with air velocity (0.47 mm copper beads, $G_p = 20$ g/s); u_a = superficial air velocity, u_p average particle velocity.

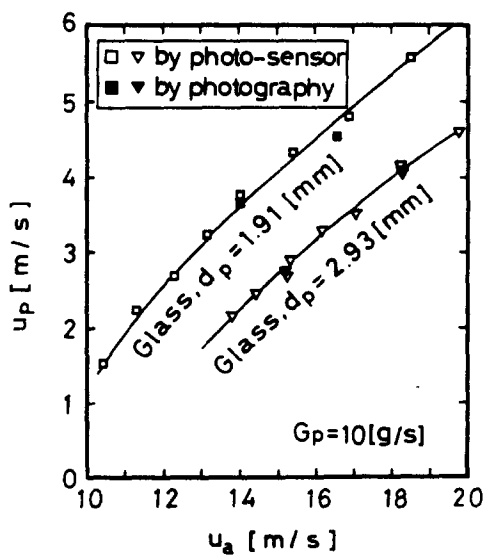

gure 6. Comparison between the mean particle velocities by this method and by the photographic method.

2.2.2 Operation of the system. The whole experimental system was supervised by a personal computer (PC8001) installed into the system. The experiment was performed by reducing the air flow rate at a constant solids flow rate. The constant flow rate of solid was attained by adjusting the vibrating feeder based on the I-PD control algorithm implemented in the personal computer, details of which was presented elsewhere (Matsumoto *et al.* 1985). The calculation of the particle velocity was also performed on-line in the computer and its result was stored on a floppy disk with other experimental conditions.

The experimental range covered in this work is up to 1.3% of volumetric concentration of solids (up to 13 of mass flow ratio of solids) and from 5 to 20 m/s of air velocity.

2.2.3 Analysis of data. Based on the observed particle velocities, friction coefficient of solids to wall and drag coefficient were evaluated as in the following, both of which are fundamental parameters in the aerodynamics of gas–solid two-phase flow. As is well known, the equations of motion for vertical gaseous suspension flow are expressed as (e.g. Soo 1982)

(gas-phase)

$$\frac{\partial u_a}{\partial t} + u_a \frac{\partial u_a}{\partial z} = -\frac{1}{\rho_a} \cdot \frac{\partial p}{\partial z} - \frac{3}{4} \cdot \frac{C_D}{d_p} \cdot \frac{\rho_{ds}}{\rho_p - \rho_{ds}} (u_a - u_p)^2 - \frac{2f_a}{D} \cdot \frac{\rho_{ds}}{\rho_p - \rho_{ds}} u_a^2 \qquad [2]$$

(solid-phase)

$$\frac{\partial u_p}{\partial t} + u_p \frac{\partial u_p}{\partial z} = -\frac{1}{\rho_p} \cdot \frac{\partial p}{\partial z} + \frac{3}{4} \cdot \frac{C_D}{d_p} \cdot \frac{\rho_a}{\rho_p} (u_a - u_p)^2 - \frac{2f_p}{D} \cdot u_p^2 - g \qquad [3]$$

where C_D is drag coefficient, f_p is friction factor of solids with wall, u_a is superficial air velocity, that is the average velocity based on the empty tube, u_p is the average particle velocity, D is tube diameter, d_p is particle diameter, ρ_a is density of gas, ρ_p is density of solid, and ρ_{ds} is the dispersed density. For steady-state fully developed flow, the left-hand sides of above equations become zero. Thus if the particle velocity and pressure gradient, $\partial p / \partial z$, were measured in the experiment, C_D and f_p can be evaluated from the above equations, because the dispersed density ρ_{ds} is a function of the solid particle velocity ($\rho_{ds} = 4G_p/(\pi D^2 u_p)$).

3. RESULTS AND DISCUSSION

3.1 Solid particle velocity

Figures 7 and 8 show the solid particles velocity as a function of superficial air velocity, which is the average air velocity based on the cross-sectional area of tube, with parameters of particle size and solids flow rate G_p. The dotted lines in the figures indicate the relative

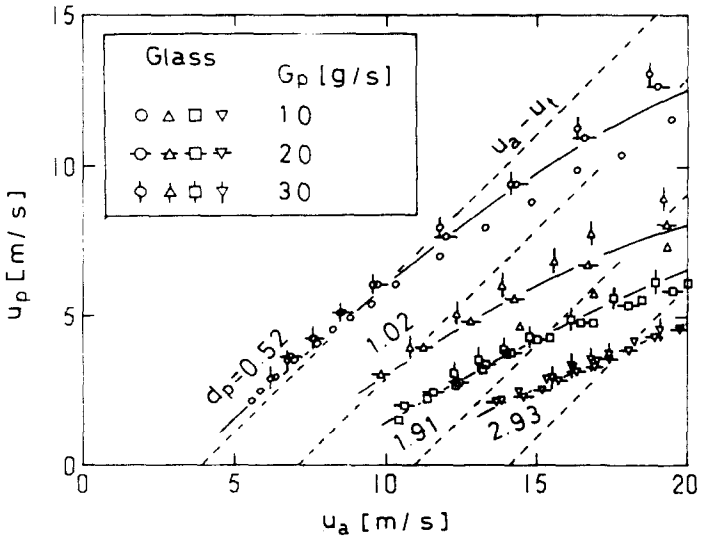

Figure 7. Particle velocity as a function of superficial air velocity.

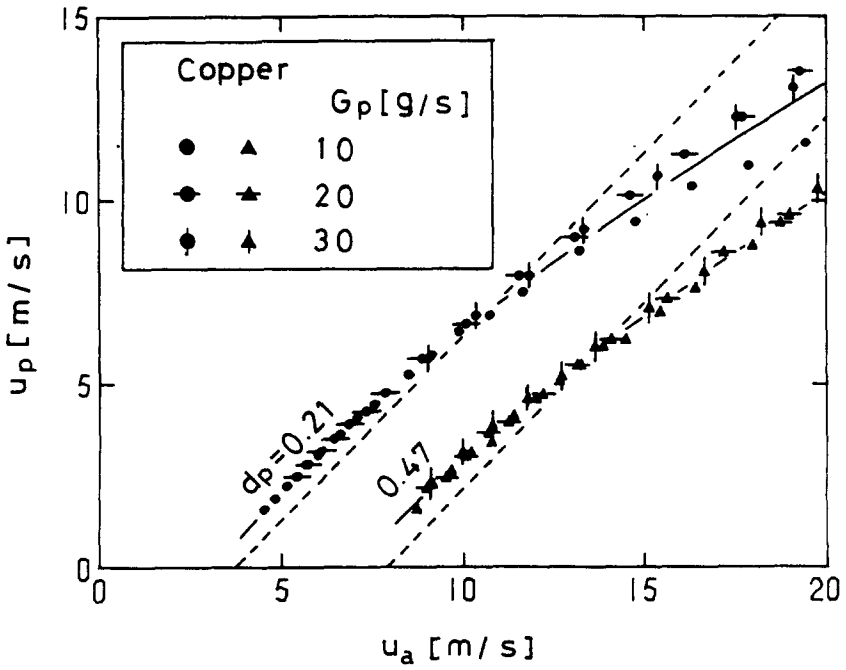

Figure 8. Particle velocity as a function of superficial air velocity.

velocity, $u_a - u_t$, calculated by subtracting the terminal velocity of a single particle based on the standard drag coefficient from the superficial air velocity. It has been usually said that this relative velocity might be a good approximation of particle velocity of suspension for very dilute concentrations (Konno & Saito 1969). It can be seen, however, that there exist two features in these figures; one is that the interpolation curves of the solid velocity intersects the dotted line. The other feature is that the solid velocities of smaller sizes of particles tend to depend on the solid flow rate as well as superficial air velocity. These features are also seen in literature (Capes & Nakamura 1973; Hariu & Molstad 1949). Capes & Nakamura (1973) explained the former feature as a result of wall-effect of conduit, but it was not so clear.

This phenomenon is understood as follows. From [3], the solid particle velocity in the fully developed flow at the steady state can be expressed in the form

$$u_p = u_a - u_t[(1+2f_p u_p^2/gD)\,(C_{D0}/C_D)]^{1/2} \qquad [4]$$

where the pressure gradient term is neglected in [3]. The symbol C_{D0} in [4] denotes the standard drag coefficient, which should be used for a single particle in infinite fluid space. Equation [4] suggests that the relative velocity between the gas and the solid increases with increasing air velocity due to the friction of particles with the wall and eventually exceeds the terminal velocity of a single particle at higher air velocities. However, at lower air velocities, the wall-effect becomes very small due to resulting small particle velocity and then the drag coefficient ratio plays an important role for the relative velocity. If the drag coefficient in suspension were greater than the standard one, then the relative velocity might be lower than the terminal velocity of a single velocity. It will result in the conclusion that the solid particle velocity would be affected by the friction due to collisions of particles with wall and drag coefficient in the suspension would be considerably greater than the standard one. Further consideration on the latter subject will be presented later on.

As for the dependence of solid particle velocity upon the solids flow rate, there is no definite explanation at the present time. This feature implies that the velocity of smaller particles is dependent upon the concentration of solids in the line as well. The fact that this effect did not appear in the results for larger particles may be attributed to the limited experimental range covered in this investigation.

3.2 Friction factor

This is usually correlated as a function of particle Froude number, $u_p/\sqrt{gD}$ (e.g. Capes & Nakamura 1973; Konno & Saito 1969). The result in this investigation, however, did not indicate a good correlation with this parameter. Now we consider what factors contribute to the friction factor. This is defined as

$$\Delta p_s = 2f_p \rho_{ds} u_p^2 L/D \qquad [5]$$

where Δp_s is pressure drop due to solids alone and L is tube length. This is based on the assumption that the suspension flow behaves as a fictitious fluid having density ρ_{ds} and causes the additional pressure drop due to friction with the wall. From another viewpoint, the additional pressure drop is mainly caused by loss of kinetic energy of particles during collisions with conduit wall. Hence the following momentum balance equation may hold

$$\Delta p_s A_c u_a = F_c \Delta E \qquad [6]$$

where A_c is the cross-sectional area of tube, F_c is the collision frequency of particle per unit time, and ΔE is the kinetic energy dissipated by collision of single particle. The amount of dissipated kinetic energy of single particle is assumed to be in proportion to the total amount of kinetic energy as,

$$\Delta E = \alpha m_p u_p^2/2 \qquad [7]$$

where m_p is mass of a single particle and α is a coefficient. The collision frequency is how frequently the particles per unit volume of tube collide with the wall, and it is considered to be in proportion to the number density of particles and the lateral component of particle velocity (Matsumoto *et al.* 1978). Provided that the lateral component is in proportion to the axial component, the collision frequency may be expressed as,

$$F_c = \beta(\rho_{ds}/m_p) A_c L u_p/D \qquad [8]$$

where β is a coefficient. Substituting [5], [7] and [8] into [6] yields

$$f_p = (\alpha\beta/4)(u_p/u_a). \qquad [9]$$

The resulting friction factor depends upon the velocity ratio u_p/u_a alone and does not involve explicitly other parameters such as tube diameter, particle size and density. In practice, the coefficients α and β may be dependent upon those parameters. Anyway, it is suggested that the friction factor would be closely related to the velocity ratio u_p/u_a. An attempt was then made to correlate f_p with the velocity ratio and the following equation was obtained;

$$f_p = 0.01(u_a/u_p)^2 Fr_t \qquad [10]$$

as shown in figure 9 where $Fr_t = u_t/\sqrt{gD}$. The difference in the exponent of u_p/u_a in [10] from that predicted by the above consideration may be due to the extreme simplification of actual phenomenon. Although the scatter of data amounts to $\pm 50\%$, it is unavoidable in this kind of quantity because of high sensitivity to the measurements of particle velocity and pressure gradient. Hariu & Molstad's (1949) data were also correlated by the above equation.

3.3 Drag coefficient

Drag coefficients obtained by the indirect measurement are plotted as a function of particle Reynolds number based on the relative velocity between superficial air and particle velocity in figure 10. The solid line indicates the standard curve calculated by the Morsi & Alexander (1972) equation. In the figure, the data by Doig & Roper (1968), Reddy & Pei (1969) and Foster *et al.* (1975) are plotted together. The results by Doig & Roper are

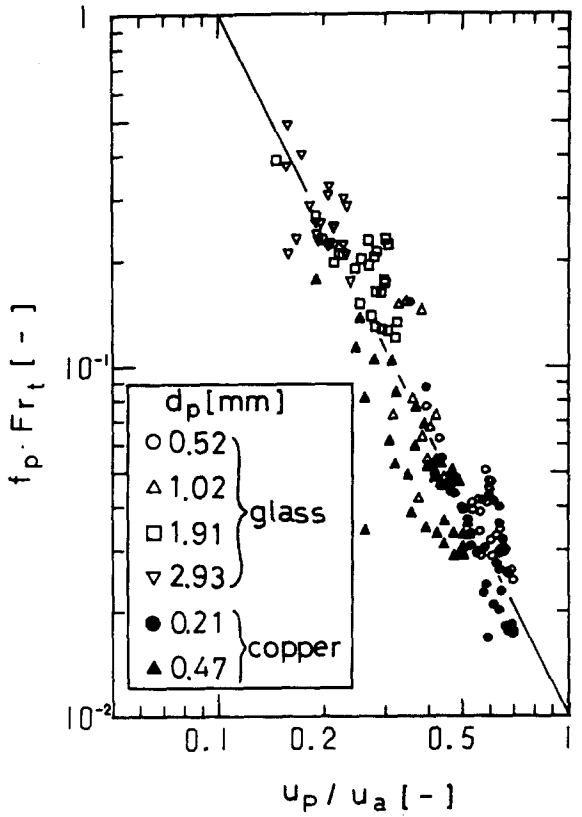

Figure 9. Correlation of friction factor ($Fr_t = u_t/\sqrt{gD}$).

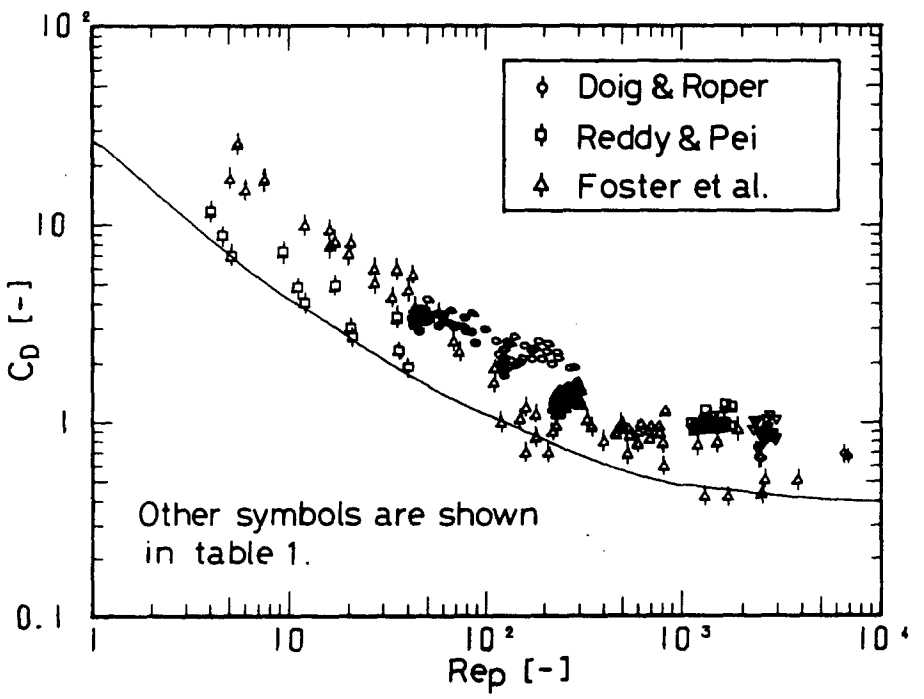

Figure 10. Observed drag coefficient as a function of particle Reynold number [$Re_p = d_p(u_a - u_p)/\nu$].

for single spheres, sizes of which range from 3.05 to 11.83 mm, suspended in a vertical riser of diameter 43 mm by an air stream, a part of which is plotted in the figure. Reddy & Pei obtained, in a similar way to this work, the average drag coefficients from the measured pressure drop due to solids alone and the relative velocity for four sizes of spherical glass beads, ranging from 0.1 to 0.27 mm, transported vertically by a turbulent air stream in a 10 cm pipe. The measurements of Foster *et al.* are for single spheres, ranging from 3.18 to 19 mm in size, suspended in a vertical pipe of diameter 69.85 mm by a sucrose solution, but the plotted data are limited to smaller sizes of particles ranging from $d_p/D = 0.069$ to 0.159.

It can be seen from the figure that the drag coefficients in this work are generally greater than the standard values. Before considering the reason for such greater values of C_D, let us examine the confidence limit of obtained values of C_D. The drag coefficient is evaluated indirectly from the measurement of pressure drop due to solids alone, mass flow rate of solids as well as average velocity of particles. Some errors are introduced in practice for these measurements, and hence those must be reflected in C_D. Now provided that the measurements of u_p, $\Delta p_s/L)$, and G_p, respectively, involve relative error δu_p, $\delta(\Delta p_s/L)$, and δG_p, then they are related to the relative error of C_D, δC_D, as follows,

$$|\delta C_D| = c|\delta u_p| + |\delta(\Delta p_s/L)| + |\delta G_p| \qquad [11]$$

where

$$c = 1 + 2u_p/(u_a - u_p) \quad . \qquad [12]$$

The value of c estimated from the experimental data ranges from about 3 to 6 for cases of smaller particles, and from 1 to 2 for larger particles. Thus the error of u_p has the most influence upon the value of C_D. If measurement error of each variable in this work would be at most 5%, then $|\delta C_D|$ becomes 0.4; that is, the obtained C_D involves uncertainty of as much as 40%. However, the actual values of C_D obtained do not have a great amount of scatter; the standard deviation of which is less than 15%. This discrepancy may be due to a pessimistic estimation of the measurement error. Judging from this point of view, it is hardly considered that such greater values of C_D are due to the measurement error alone. That is, though the accuracy may not be so high, it can be inferred from the above consideration that the drag coefficients for suspension are certainly greater than the standard coefficients.

Richardson & Zaki (1954) examined experimentally the effect of concentration of suspended particles and the size ratio d_p/D upon the terminal velocities of suspensions by using liquid–solid fluidization. Their results, rearranged into the drag coefficient ratio, are summarized as follows,

$$C_D/C_{D0} = \epsilon^{-2n} \cdot 10^{2(d_p/D)} \qquad [13]$$

where ϵ is a void fraction and n is a function of Re_p and d_p/D. This correlation suggests that the effect of solid concentration is not so noticeable under the experimental conditions concerned since the voidage is always greater than 0.986 and hence the value of ϵ^{-2n} does not exceed 1.07. On the other hand, the wall-effect is more pronounced as shown in the following; the value of d_p/D ranges from 0.0105 to 0.1465 in this work and the resulting value of wall-effect term ranges from 1.05 to 1.96. Combining the above two effects yields the value of C_D/C_{D0} ranging from 1.12 to 2.06. Especially, for the largest size of particles, that is 2.93 mm glass beads, $C_D/C_{D0} = 2.06$, which is consistent with the increase of drag coefficient in this work. Results by Foster *et al.* are also interpreted similarly because those were obtained for relatively large values of d_p/D as shown above. Actually, they explained that such a remarkable increase of C_D resulted from the deformation of fluid velocity profile due to the wall-effect. On the other hand, the wall-effect may not be pronounced in Reddy & Pei's experiments because they used relatively small particles ($0.001 \leq d_p/D \leq 0.0027$). Nevertheless, Reddy & Pei's data show somewhat greater values than the standard ones.

They inferred that it might be due to the effect of fluid turbulence. As for the effect of turbulence on the drag coefficient, Clift & Gauvin (1971) presented a comprehensive review. It is pointed out in the review that fluid turbulence can change the drag coefficient markedly in various ways and its effect is characterized by the relative intensity $I_R = \sqrt{\overline{u'^2}}/u_R$ where u' is fluctuation of fluid velocity and u_R is slip velocity. Since no turbulence characteristics were measured in this work, it is impossible to evaluate the magnitude of I_R and to estimate its effect exactly. However, it is suggested that the drag coefficient for suspension might be increased up to twice that of the standard one, if I_R were around 0.4 at intermediate particle Reynolds numbers ($50 \leq \mathrm{Re}_p \leq 700$).

Finally, it can be inferred from the above consideration that remakable increase of C_D in this work may be due to the wall-effect and influence of fluid turbulence. Particularly, the former effect may be dominant for larger particles. For the results observed here alone, the following correlation was obtained:

$$C_D/C_{D0} = 3.02\,(\mathrm{Re}/\mathrm{Re}_p)\,(d_p/D)^{1.27} \qquad [14]$$

as shown in figure 11 where $\mathrm{Re} = Du_a\rho_a/\mu$.

3.4 Correlation of particle velocities

Substitution of [10] into [4] suggests that the particle velocity seems to be correlated by a nondimensional parameter Fr^2/Fr_t as the drag coefficient ratio in [4] is almost constant. Under this view, the following correlation was obtained;

$$\frac{u_a - u_p}{0.71u_t} = (1 + 0.0065 \cdot Fr^{2.5}/Fr_t^{1.25})^{1/2} \qquad [15]$$

as shown in figure 12 where $Fr = u_a/\sqrt{gD}$. Most points are seen to lie within $\pm 20\%$ except some data of 1.02 mm glass. Comparisons of Konno & Saito's (1969), and Hariu & Molstad's (1949) data with [15] are shown in figures 13 and 14. Konno & Saito's data are satisfactorily correlated by [15], despite the fact that those were obtained with larger sizes of tube (D =26.5 and 46.8 mm). On the other hand, Hariu & Molstad's data (figure

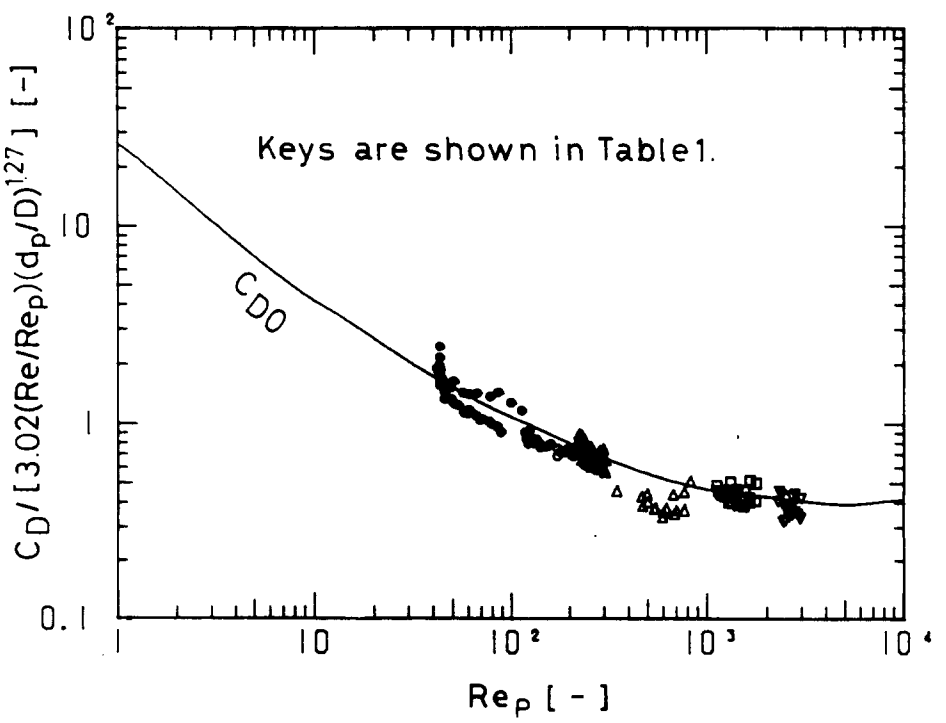

Figure 11. Correlation of drag coefficient ($\mathrm{Re} = Du_a\rho_a/\mu$).

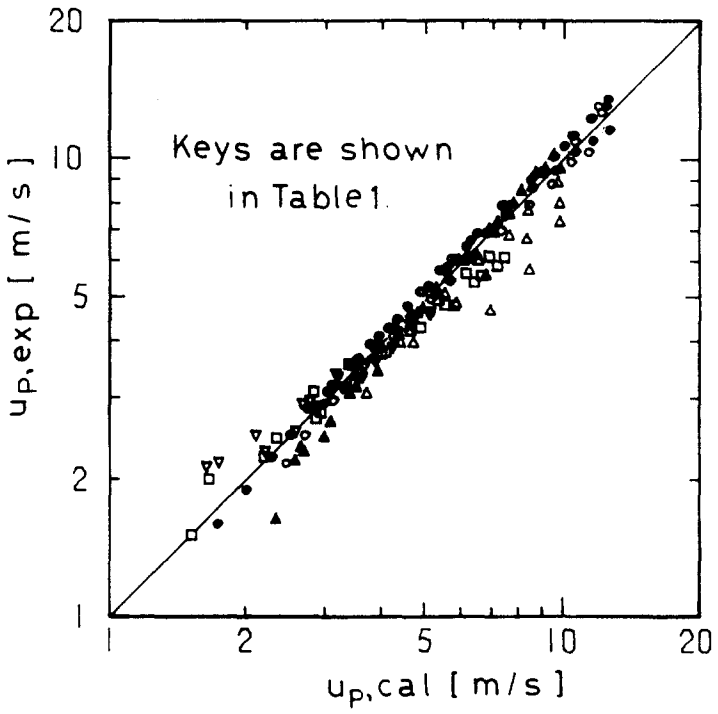

Figure 12. Comparison of calculated particle velocities by [15] with observed ones.

14) are somewhat smaller than the predicted values by [15]. This is probably due to the fact that those were obtained by use of short transport lines (their lengths were 1.2 and 1.5 m) not enough for full acceleration of particles and the particles used were sand, not spherical, whereas [15] was based on the results with spherical particles.

4. CONCLUSIONS

It was shown that the proposed method could be applied to the measurement of the mean solid velocity in the transport line and also had advantages of low cost and on-line measurement. The apparent relative velocity of superficial air- to mean solid velocity, in the vertical suspension flow exhibited such complicated behaviors that it was smaller than the terminal velocity of a single particle at lower air velocities but greater at higher velocities.

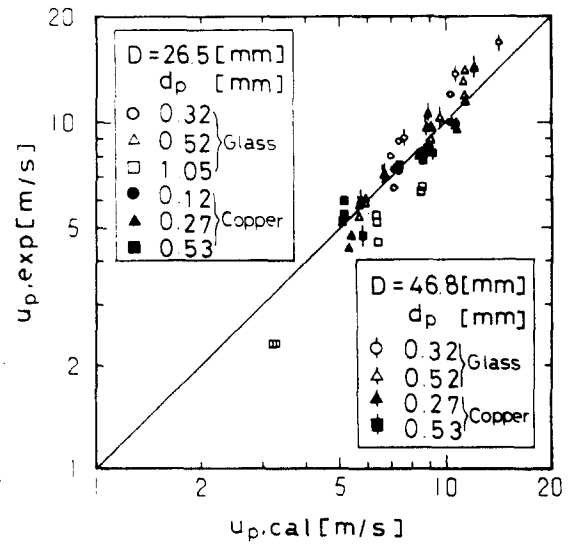

Figure 13. Comparison of calculated particle velocities by [15] with Konno & Saito's (1969) data.

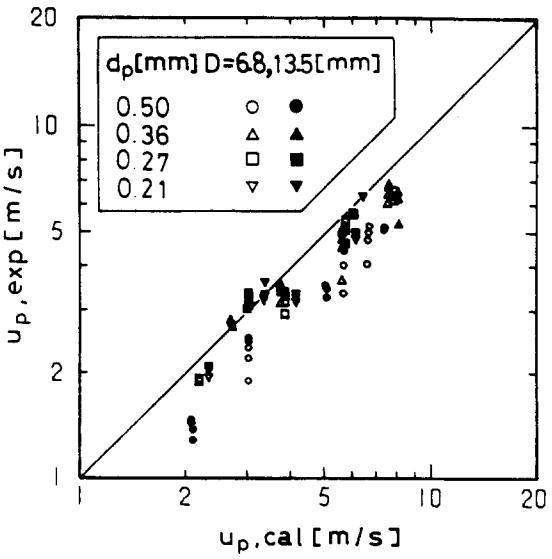

Figure 14. Comparison of calculated particle velocities by [15] with Hariu & Molstad's (1949) data.

These were explained as a combined result of contribution of solid friction with conduit wall and greater value of drag coefficient in the suspension. The particle velocities were satisfactorily correlated by [15], by which the literature data also correlated well despite varieties of tube and particle sizes.

Acknowledgement—The authors wish to express their thanks to the Science Research Foundation of the Ministry of Education, Science and Culture, Japan, for its financial support (Grant No. 59550639).

REFERENCES

BECK, M.S., DRANE, J., PLASKOWSKI, A. & WAINWRIGHT, N. 1969 Particle velocity and mass flow measurement in pneumatic conveyers. *Powder Technol.* **2**, 269–277.

CAPES, C.E. & NAKAMURA, K. 1973 Vertical pheumatic conveying: An experimental study with particles in the intermediate and turbulent flow regimes. *Can. J. Chem. Eng.* **51**, 31–38.

CLIFT, R. & GAUVIN, W. H. 1971 Motion of entrained particles in gas streams. *Can. J. Chem. Eng.* **49**, 439–448.

DOIG, I.D. & ROPER, G.H. 1968 Contribution of the continuous and dispersed phases to the suspension of spheres by a bounded gas–solids stream. *Ind. Eng. Chem. Fundam.* **7**, 459–471.

FOSTER, B.P., HAIR, A.R. & DOIG, I. 1975 Suspension of spheres in fully developed pipe flow. *Chem. Eng. J.* **9**, 241–249.

HARIU, O.H. & MOLSTAD, M.C. 1949 Pressure drop in vertical tubes in transport of solids by gases. *Ind. Eng. Chem.* **41**, 1148–1160.

IRONS, G.A. & CHANG, J.S. 1983 Particle fraction and velocity measurement in gas–powder streams by capacitance transducers. *Int. J. Multiphase Flow* **9**, 289–297.

KONNO, H. & SAITO, S. 1969 Pneumatic conveying of solids through straight pipes. *J. Chem. Eng. Japan* **2**, 211–217.

LEE, S.L. & SRINIVANSAN, J. 1978 Measurement of local size and velocity probability density distributions in two-phase suspension flows by laser-Doppler technique. *Int. J. Multiphase Flow* **4**, 141–155.

LEE, S.L. & SRINIVANSAN, J. 1982 An LDA technique for *in situ* simultaneous velocity and size measurement of large spherical particles in a two-phase suspension flow. *Int. J. Multiphase Flow* **8**, 47–57.

LÜBBESMEYER, D. & LEONI, B. 1983 Fluid-velocity measurements and flow-pattern identification by noise analysis of light-beam signals. *Int. J. Multiphase Flow* **9**, 665–679.

MATSUMOTO, S., OHNISHI, S. & MAEDA, S. 1978 Heat transfer to vertical gas–solid suspension flows. *J. Chem. Eng. Japan* **11**, 89–95.

MATSUMOTO, S., SATO, H., SUZUKI, M. & MAEDA, S. 1982 Prediction and stability analysis of choking in vertical pneumatic conveying. *J. Chem. Eng. Japan* **15**, 440–445.

MATSUMOTO, S., HARAKAWA, H., SUZUKI, M. & OHTANI, S. 1985 The control of solid flow rate in a pneumatic conveyer. *J. Soc. Powder Technol.*, Japan **22**, 3–10 (in Japanese).

MORSI, S.A. & ALEXANDER, A.J. 1972 An investigation of particle trajectories in two-phase flow systems. *Fluid Mech.* **55**, 193–208.

REDDY, K.V.S. & PEI, D.C.T. 1969 Particle dynamics in solids–gas flow in a vertical pipe. *Ind. Eng. Chem. Fundam.* **8**, 490–497.

RICHARDSON, J.F. & ZAKI, W.N. 1954 Sedimentation and fluidisation: Part I. *Trans. Instn. Chem. Engrs.* **32**, 35–53.

SOO, S.L. 1982 Fluid mechanics of suspensions. *Handbook of Multiphase Systems* (Edited by G. HETSRONI), pp. 3.6–3.10. Hemisphere, Washington, D.C.